INTERNATIONAL JOURNAL OF AUTOMOTIVE AND MECHANICAL ENGINEERING (IJAME)
ISSN: 2229-8649 e-ISSN: 2180-1606
VOL. 18, ISSUE 3, 9082 – 9093
DOI: https://doi.org/10.15282/ijame.18.3.2021.20.0697

ORIGINAL ARTICLE

Performance of Combustion and Emissions Characteristics of Ethanol Dual Injection Spark Ignition Engine

N.F.O. Al-Muhsen[1,*], G. Hong[2] and F.B. Ismail[3]

[1]Middle Technical University, Baghdad, 10001 Iraq
[2]School of Mechanical and Mechatronic Engineering, University of Technology Sydney, 15 Broadway, Ultimo, NSW, 2007, Australia
[3]Power Generation Unit, Institute of Power Engineering (IPE), Universiti Tenaga Nasional (UNITEN), 43000 Kajang, Selangor, Malaysia

ABSTRACT – Ethanol dual injection (DualEI) is a new technology to maximise the benefits of ethanol fuel to the spark-ignition engine. In this study, the combustion and emissions characteristics in a DualEI spark-ignition engine with a variation of the direct injection (DI) ratio and engine speed were experimentally investigated. The volume ratio of DI was varied from 0% (DI0%) to 100% (DI100%), and two engine speeds of 3500 and 4000 RPM were tested. The spark timing for maximum brake torque (MBT) was first determined, and then the results of the effect of DI ratio on the engine performance at the MBT conditions were discussed and analysed. The results showed that the MBT timing for the DI and spark timings were 330 and 30 CAD bTDC, respectively. At the MBT timing, the indicated mean effective pressure slightly increased from 0.47 to 0.50 MPa when the DI ratio increased from DI0% to DI100%. However, the maximum combustion pressure significantly decreased by 8.32%, and volumetric efficiency increased by 4.04%. This was attributed to the reduced combustion temperature due to the cooling effect of ethanol fuel enhanced by the DI strategy. The indicated specific carbon monoxide and hydrocarbons significantly increased due to poor mixture quality caused by fuel impingement associated with the overcooling effect. However, the indicated specific nitric oxides significantly decreased due to the temperature reduction inside the combustion chamber. Results showed the potential of DualEI to increase the compression ratio and consequently increase the engine thermal efficiency without the risk of engine knock.

ARTICLE HISTORY
Received: 26th June 2020
Revised: 5th Sept 2021
Accepted: 16th Sept 2021

KEYWORDS
Spart ignition engine;
Ethanol dual combustion;
Ethanol combustion;
Emissions

NOMENCLATURE

bTDC	before top dead centre
CAD	crank angle degree
CA10-90%	the major combustion duration
CA50	combustion phase when 50% of the fuel is burnt
DI	direct injection
DIT	direct injection timing
DualEI	ethanol dual-injection
EPI	ethanol port injection
GDI	gasoline direct injection
HRR	heat release rate
IMEP	indicated mean effective pressure
ISCO	indicated specific carbon monoxide
ISFC	indicated specific fuel consumption
ISHC	indicated specific hydrocarbon
ISNO	indicated specific nitric oxide
MBT	minimum spark advance for best torque
P_{max}	maximum cylinder pressure
λ	air/fuel equivalent ratio (lambda)

INTRODUCTION

The ever increasingly tightened regulations have been enforced to reduce emissions produced by internal combustion (IC) engines. The research about improving the engine performance has been led by two main respects, which are exhaust emission reduction and fuel economy improvement. Compared to Euro 3, Euro 6 have lowered the nitric oxide (NO), carbon monoxide (CO) and hydrocarbon (HC) emissions limits by 60%, 57% and 50% for light-duty cars respectively [1]. Alcohol-fueled spark ignition engine (SI engine) is an option to reduce the greenhouse gas emissions produced from

*CORRESPONDING AUTHOR | Nizar F.O. Al-Muhsen | ✉ nizar.almuhsen@mtu.edu.iq

gasoline-fueled engines. Ethanol fuel has been used globally as an additive and/or an alternative fuel to fossil fuel in SI engines to address the issue of sustainability [2]. Ethanol is a renewable fuel that can offset its carbon dioxide (CO_2) impact because it is produced from a range of bio-resources. Consequently, this possibly leads to a partially virtuous production-consumption cycle. Compared to gasoline, ethanol has a greater flame speed, octane number, and heat of vaporisation, and it provides cleaner combustion [3, 4]. Furthermore, ethanol has lower stoichiometric air to fuel ratio, smaller adiabatic flame temperature and the much greater latent heat of vaporisation (cooling effect), which could result in lower combustion temperature and thus less convective heat losses [5, 6]. On the other hand, ethanol has a lower heating value, which consequently increases the mileage fuel consumption compared to gasoline [6, 7]. Slow evaporation rate at low ambient temperature, lower vapour pressure, and heating value are also reported to ethanol fuel as an issue of cold starting [8, 9]. As a result, flex-fuel systems were widely used as auxiliary system to aid SI engine cold starting by using gasoline port injection (GPI) [10]. Flex-fuel systems were widely used in the US and South America, such as Brazil, to reduce CO_2 emission by transferring the SI engines from gasoline-fueled to be 100% ethanol engines [11-13]. However, the flex-fuel vehicles mostly were equipped with conventional port fuel injection systems resulting in moderate engine performance and relatively poor mileage fuel economy.

Controlling the mixture formation processes inside the combustion chamber can be a key parameter to improve the engine performance. Yu et al. blended different types of fuels with ethanol aiming to optimise the combustion phasing to enhance SI engine thermal efficiency [14]. The authors adopted many fuels and dual injection strategies in their experimental investigation. The hydrogen was directly injected into the cylinder to overcome the slow evaporation rate and high latent heat of vaporisation of ethanol fuel that port injected. The combustion quality was enhanced, IMEP was increased, and combustion emissions (HC and CO) were decreased when the hydrogen fuel was used with ethanol. On the other side, Habib et al. [15] port-injected the ethanol fuel in a compression engine in order to improve the combustion performance of diesel fuel. Their engine was tested at different engine speeds and energy ratios of ethanol fuel. The authors' results showed that output brake power was improved and the NOx emissions decreased, but the HC and CO emissions were increased. Similar outcomes were attained by Qian et al. [16] as they investigated the effect of the volume ratio of ethanol fuel port injection on the combustion and emissions performance. The engine knock limit was advanced with an increased ratio of ethanol fuel due to the high cooling effect of ethanol fuel caused by the large ethanol latent heat of vaporisation [17]. This could potentially reduce the combustion chamber temperature increasing the engine knock limits.

Although ethanol is considered an environmentally friendly fuel due to its green production to consumption cycle [18], adopting ethanol fuel as an alternative fuel to fossil fuel such as gasoline could come with considerable challenges [19]. Nakata et al. and Taniguchi et al. [12, 20] from Toyota Motor Company investigated the feasibility of running the SI engine with 100% ethanol. They concluded that ethanol could improve the engine thermal efficiency due to the greater octane number and cooling effect compared to the standard unleaded gasoline. It was reported that 100% ethanol direct injection (EDI) could significantly improve the engine performance and reduce the NO emission [21, 22]. However, the results showed that the over-cooling effect associated with the severe fuel impingement due to a high percentage of EDI ratio were represented as possible issues to the SI engines [17]. The Ethanol dual injection (DualEI) system could simultaneously control the amount of ethanol port injected to directly injected based on the engine needs. Using a high-pressure DI unit plus ethanol fuel could potentially reduce the consequent emissions. Greater injection pressure could produce finer droplets and less fuel impingement.

Zhuang et al. [23, 24] investigated the merits of the EDI on a GPI engine. It was reported that the combustion performance was significantly improved when EDI was used. Huang et al. numerically investigated the combustion and emissions characteristics [8, 17]. The results showed that the engine performance slightly improved due to injecting a certain amount of ethanol directly into the combustion chamber. Further increase in the EDI ratio over 60% deteriorated the combustion quality due to the ethanol impingement and the over-cooling effect. The greater laminar flame speed combined with oxygen content helped in enhancing the combustion quality. A significant reduction in the NO emission occurred due to the ethanol lower adiabatic flame temperature and the cooling effect of the EDI. However, HC and CO emissions increased considerably. This was attributed to the rich mixture regions, mainly ethanol wall film, created inside the combustion chamber when a high ratio of EDI was used. Zhu et al. [25] tested the effect of different ethanol-gasoline dual-injection techniques on the combustion characteristics. GPI plus EDI and ethanol port injection plus gasoline direct injection (EPI+GDI) strategies were included. The best combustion performance was recorded at GPI+EDI that the indicated mean effective pressure (IMEP) increased by 2% at light engine load.

As discussed above, adopting biofuel such as ethanol presents new challenges to engine development. Even though different technologies have been used recently to exploit the benefits of ethanol, fossil fuel like gasoline is still the main fuel for IC engines. DualEI is a new technology under development aiming to exploit the benefits of using pure ethanol as an alternative fuel to SI engines. This paper aims to investigate the effect of the volume DI ratio on combustion and emissions characteristics of a naturally aspirated SI engine equipped with a DualEI system. An investigation of the effects of the DI and spark timings were also involved at the beginning, so the spark timing for maximum brake torque (MBT) timing can be achieved.

EXPERIMENTAL APPARATUS AND METHODOLOGY

Engine Setup

The experiments were performed on a modified Yamaha YBR250 motorcycle engine, as shown in Figure 1. The engine is a single-cylinder four-stroke air-cooled naturally aspirated SI engine. Table 1 shows the major specifications of the research engine. The engine was originally equipped with a GPI system before it was modified to be equipped with a DualEI system by Hents Technology to meet the research needs. The engine modification included the installation of a direct fuel injection system and an electronic control unit (ECU) which was used to control the throttle position, spark timing, DI timing, and pressure and the injection duration per cycle. The DI system is comprised of a returnless high-pressure pump and a six-hole high-pressure injector [26]. The injector was side-mounted between the intake valve seat and the spark plug [24]. The slope angles of the injector are 15º from the horizontal surface of the cylinder head to the axis of the injector and 12º from the vertical surface of the cylinder head. Table 2 shows the major specifications of the direct fuel injector. More details about the nozzle plume bend angles and their distribution can be found in reference [9].

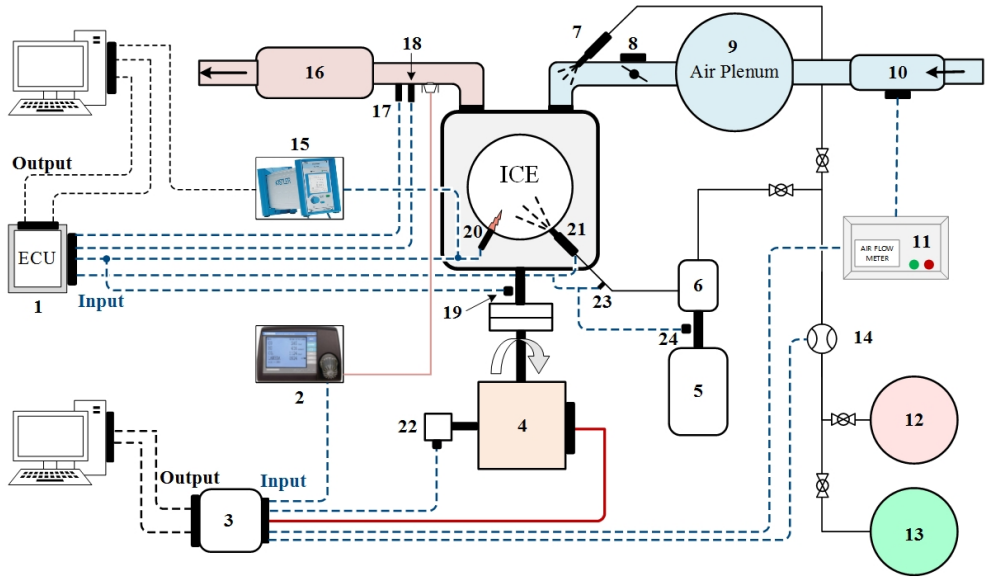

1. Electronic Control Unit (ECU) 2. Horiba MXEA-584L Exhaust Gas Analyser 3. NI-Module and Dynamometer Controller 4. Eddy Current Dynamometer 5. Electrical Motor 6. High Pressure Fuel Pump 7. Low Pressure Fuel Injector 8. Step Motor and Throttle Valve Position Sensor 9. Intake Air Stabiliser (Air Plenum) 10. Intake Air Flow Sensor 11. TOCEIL Air Flow Meter 12. Unleaded Gasoline Tank 13. Pure Ethanol Tank 14. Super Micro M-39 Fuel Flow Meter 15. KISTLER-5015A Charge Amplifier 16. Exhaust Gas Catalyser 17. K-Type Thermocouple 18. Bosh Wide-Band Lambda Sensor 19. Crank Shaft Encoder 20. KISTLER-6115B Spark Plug Pressure Transducer 21. High Pressure Fuel Injector 22. S-Type Load Cell 23. Common Rail High Pressure Sensor 24. High Pressure Fuel System Encoder

Figure 1. DualEI engine schematic diagram.

Table 3 lists the technical properties of the used measurement apparatuses. A super-micro oval fuel flow meter with ±5 ml accuracy was used to measure the ethanol fuel flow rates of port and direct injections. An eddy current dynamometer was used to control the engine speed and measure the torque. A Kistler 6115B spark plug pressure transducer and a Kistler 5011 charge amplifier were used to recording the in-cylinder pressure. K-type thermocouples were used to measure the cylinder head temperature and exhaust gas temperature with a resolution of 0.1 ºC and uncertainty of 0.35%. A MEXA-584L Horiba exhaust gas analyser was used to measure the exhaust gas emissions of CO, CO_2, HC, NO and lambda (λ). The H/C and O/C ratios were manually set in the exhaust gas analyser to be 3.0 and 0.5, respectively. The intake airflow was stabilised in an 80L intake buffer tank, and the intake air flow rate was measured using a ToCeiL20N thermal air-mass flow meter.

Table 1. Specifications of the dual ethanol research engine.

Engine type	Single cylinder, 4-stroke, SOHC
Displacement	249.0 cc
Bore	74.0 mm
Stroke	58.0 mm
Compression Ratio	9.8:1
Intake Valve Open (IVO)	382.2 CAD bTDC
Intake Valve Close (IVC)	126.2 CAD bTDC
Exhaust Valve Open (EVO)	594.6 CAD bTDC
Exhaust Valve Close (EVC)	340.7 CAD bTDC

Table 2. Specifications of the direct fuel injector [27, 28]

Manufacturer	Bosch
Operating pressure	Up to 500 bar
Number of holes	6 holes
Hole diameter	110 µm
Flow rate @ 100 bar	Up to 1640 g/min
Spray angle single beam	17°
Operating temperature range	-31 to 130 °C

Table 3. Technical properties of the used measurement apparatuses.

Measurement devices	Technical properties	Accuracy
Thermocouples: - Inlet air temperature - Exhaust gas temperature - Engine body temperature	K-type thermocouple	± 0.1 °C
Fuel flow meter	Super-micro-M-39	± 5.0 ml
In-cylinder pressure [29]	Kistler 6115B pressure transducer via a Kistler 5011 charge amplifier.	maximum measurement error of ±0.5%
Intake airflow [29]	ToCeil20N hot-wire thermal air-mass flow meter	maximum measurement error of ±1.0%
Lambda sensor [29]	Bosch (wide-band lambda sensor)	± 1.0%

Experimental Conditions and Methodology

GPI strategy was used for starting and heating up the DualEI engine until the cylinder head temperature became stable at around 200 °C (±3). Then GPI was switched to ethanol port injection, and the air/fuel ratio was kept at the stoichiometric condition (λ≈1). The experimental engine conditions are listed in Table 4. The current investigation consists of two stages of experimental works. The first experimental set aims to find the MBT timing at a range of DI and spark timings. The volume ratio of the ethanol DI to ethanol port injection was defined as DIXX%, which was fixed at around 50% in the first experiment set. The MBT timing was determined for the best IMEP and least emissions. While the second experimental set was conducted at the MBT timing from the first stage. The direct injection (DI) ratio was varied from DI0.0% (port injection only) to DI100% (direct injection only) at light load (22% ± 1% throttle position). The engine speed was set at around 3500 and 4000 RPM (±50 RPM). The DI timing was varied from 240 to 330 CAD bTDC with 30 crank angle degree (CAD) increment. The spark timing was swept from 28 to 34 CAD bTDC with 2.0 CAD increment.

Table 4. Experimental operating conditions.

First set:	
Engine loads	Light load (22% throttle opening)
Engine speed	3500 RPM
Spark timing	28, 30, 32, 34 CAD bTDC
Direct injection ratio	DI50%
Port fuel injection timing	410 CAD bTDC
Direct injection timing	240, 270, 300, 330 CAD bTDC
Second set:	
Spark and DI timings	MBT timing (ST30, DIT330)
Engine speed	3500 and 4000 RPM
DI ratio	From DI0% to DI100%

A LabVIEW code was home-developed to record the engine data at each tested engine operation condition. Five samples were recorded at a sample rate of 1 Hz, and the average values were used in the calculations and analyses. The in-cylinder pressure data was recorded independently at 0.5 CAD resolution with 100 consecutive cycles in each sample. The ensemble average of the cylinder pressure data was used in analysing the engine performance and the combustion characteristics. The maximum standard deviations of the measurements were 6.8% for indicated specific carbon monoxide (ISCO), 7.1% for indicated specific nitric oxide (ISNO) and 3.7% for indicated specific hydrocarbons (ISHC), which showed an acceptable quality of the experimental data. To determine the MBT timing, the best output power, combustion quality and minimum produced emissions were experimentally investigated and analysed. Consequently, the spark timing was set at 30 CAD bTDC, and the DI timing was set at 330 CAD bTDC for the main experiment.

RESULTS AND DISCUSSION

Engine Performance and Combustion Characteristics at MBT Window

In this work, the MBT window for this DualEI engine was experimentally determined at four sparks and DI timings, which are more likely to produce the maximum output power with the best combustion quality [30]. The DI timings (DIT) were set directly after the exhaust valve closed, which were DIT240, DIT270, DIT300, and DIT330. At each DI timing,

four spark timings (ST) were tested and specified as ST28, ST30, ST32, and ST34. The engine speed was 3500 RPM and DI ratio of 50% at light engine load. In the result analysis, the CA50 is defined as the centre of the combustion phase, and it was measured in CAD where half of the fuel mass burnt. The major combustion duration (CA10-90%) was defined as the time required to consume 90% of the fuel mass used per cycle starting from the CAD where 10% to 90% of the used fuel has burnt.

Figure 2 shows the engine performance and combustion characteristics results represented by the CA50 and CA10-90%. As shown in Figure 2(a), the DIT330 shows the greatest IMEP for all the selected spark timings compared to that of DIT240 timing. Consequently, the same performance is observed for the indicated thermal efficiency due to the fixed amount of injected fuel per cycle, as shown in Figure 2(b). This performance could be attributed to the sufficient time that is available to the air and fuel to be homogeneously mixed before the combustion starts. Furthermore, at DIT330, the residuals and the hot combustion chamber walls might be utilised to improve ethanol's evaporation process, improving the mixture quality. The combustion stability represented by the coefficient of variation of the IMEP (COV_{IMEP}) was investigated and analysed based on in-cylinder pressure, which was recorded at 100 consecutive cycles with a resolution of 0.5 CAD. The COV_{IMEP} for all the engine conditions was within the acceptable limit which is less than 10% [31]. The minimum value of the COV_{IMEP} was recorded at DIT330 for all the tested spark timings in the MBT window, as shown in Figure 2(c).

For a further understanding of the engine performance results, the combustion characteristics including the combustion angle (CA50) and combustion duration (CA10-90%) were calculated and analysed based on the recorded in-cylinder pressure. The CA50 advances toward the top dead centre and CA10-90% significantly decreases when the spark timing was advanced, as shown in Figure 2(d) and 2(e). From the DI timing vs spark timing window, achieving the best results at DI timing of 330 CAD bTDC could be attributed to two main reasons. Firstly, the early injection timing provides more time for ethanol to be evaporated and homogeneously mixed with air before the ignition starts. This might significantly improve the mixture quality and then the combustion performance. Secondly, the hot residuals and the hot combustion chamber parts such as the piston surface and exhaust valve could be fully utilised in improving the evaporation rate of ethanol due to injecting the fuel just after the exhaust valve closed. This could significantly accelerate the slow evaporation rate of ethanol and enhance the air-fuel mixing process [32]. Moreover, impinging fuel, which is directly injected, into hot surfaces could not only enhance the evaporation of ethanol but also might reduce the fuel film formation on the combustion chamber surfaced. Consequently, rich mixture regions could be avoided, and this could significantly contribute in a more evenly distributed mixture inside the combustion chamber.

Further investigation to the combustion characteristics at the MBT window, the in-cylinder pressure trace and the heat release rate (HRR) were experimentally investigated, as shown in Figure 3. The peak pressure and the maximum heat release rate increased when the DI and spark timings were advanced. In addition, the phase of the maximum pressure and the maximum heat release rate were advanced when the spark and DI timing were advanced. For instance, at ST30, the HRR increases when the DI timing is advanced from DIT240 to DIT330. Similarly, the peak pressure increases significantly with advanced DI timing.

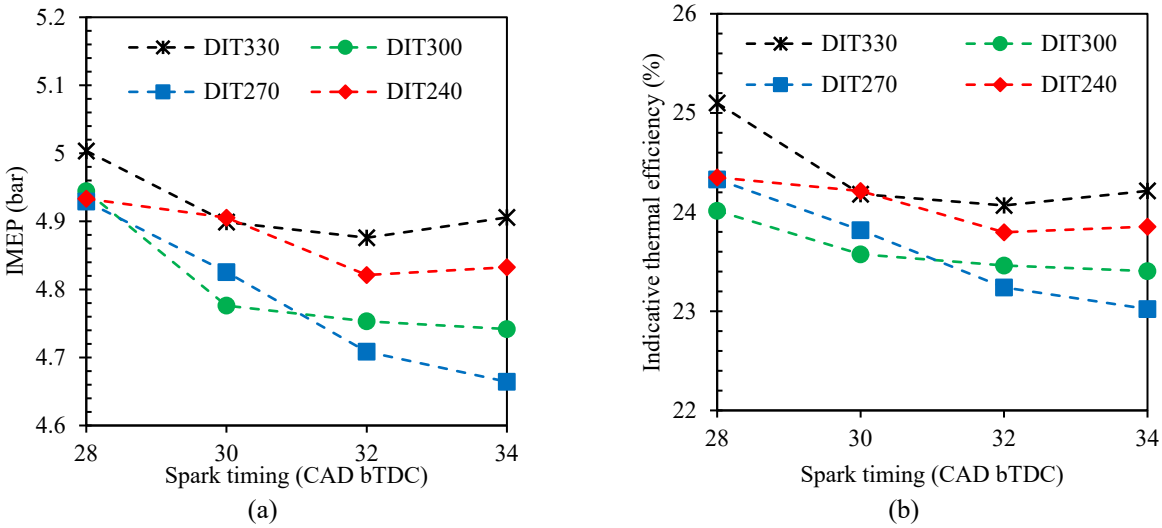

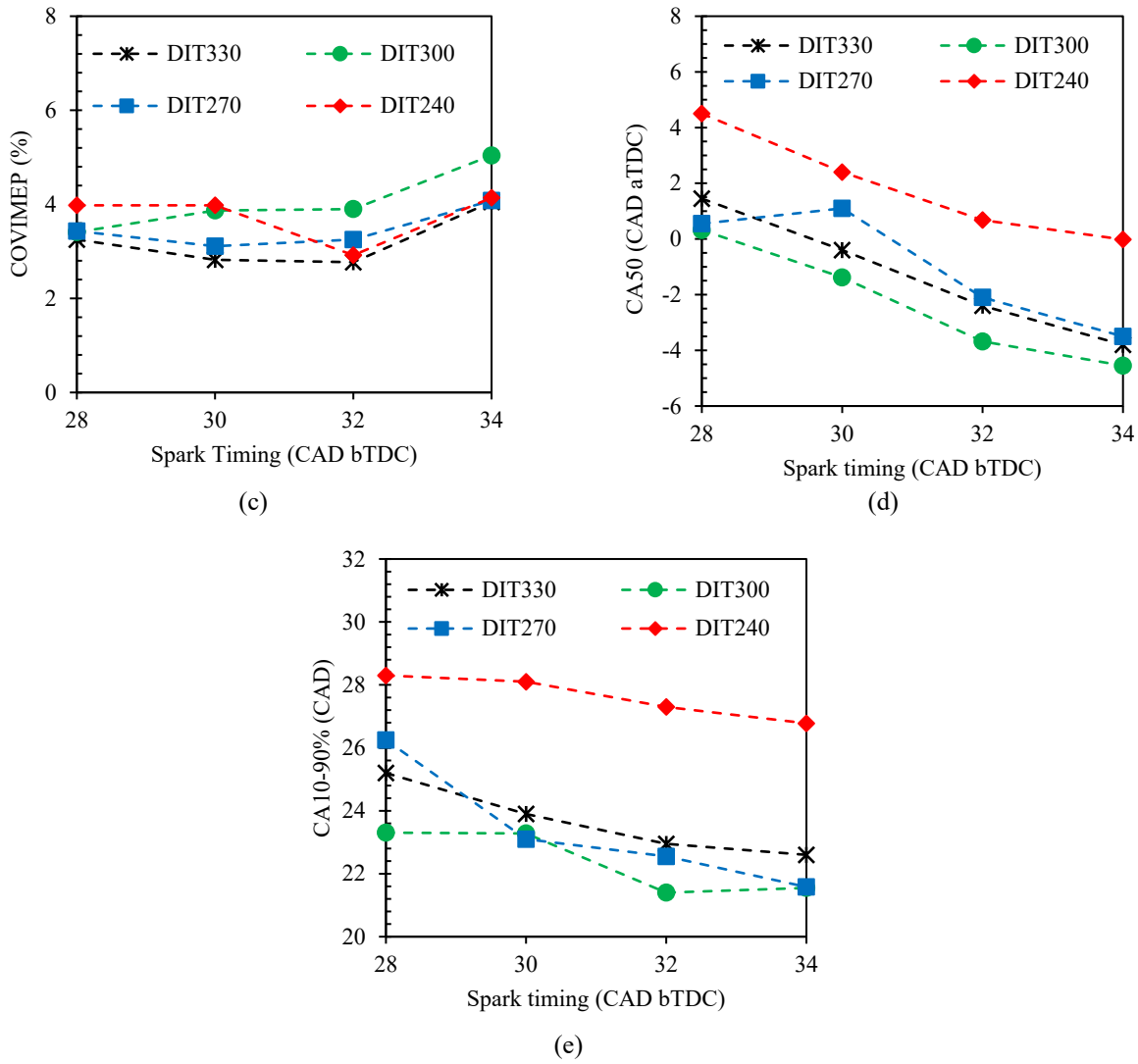

Figure 2. (a) IMEP, (b) indicative thermal efficiency, (c) the coefficient of variation of the IMEP and (d), (e) combustion characteristics (CA50 and $\theta_{10\text{-}90\%}$) variation with DI and spark timings.

Furthermore, the phases of the maximum pressure and the HRR also advanced toward the TDC when the DI and spark timings were advanced. It was reported that the DI and spark timings worked interactively together on enhancing the air-fuel mixture quality and then improving the combustion performance [30]. The DI timing of 330 CAD bTDC shows the best engine performance and combustion stability. The improvement in the engine performance could be mainly attributed to the improvement in the mixture and combustion quality. At DIT330, the ethanol is directly injected at the beginning of the intake stroke when the intake valve is nearly fully opened, and the flow velocity of the air-ethanol mixture inlet is faster compared to DIT240. This might enhance the vapour pressure of ethanol and thus promote the mixing process with air. Also, as a result of a cooling effect caused by the DI strategy, the fresh mixture temperature can decrease significantly due to an early DI timing, resulting in greater engine's volumetric efficiency and consequently enhanced combustion quality [23]. This could partly explain the improvement in the engine and combustion performance, as shown in Figure 2 and Figure 3.

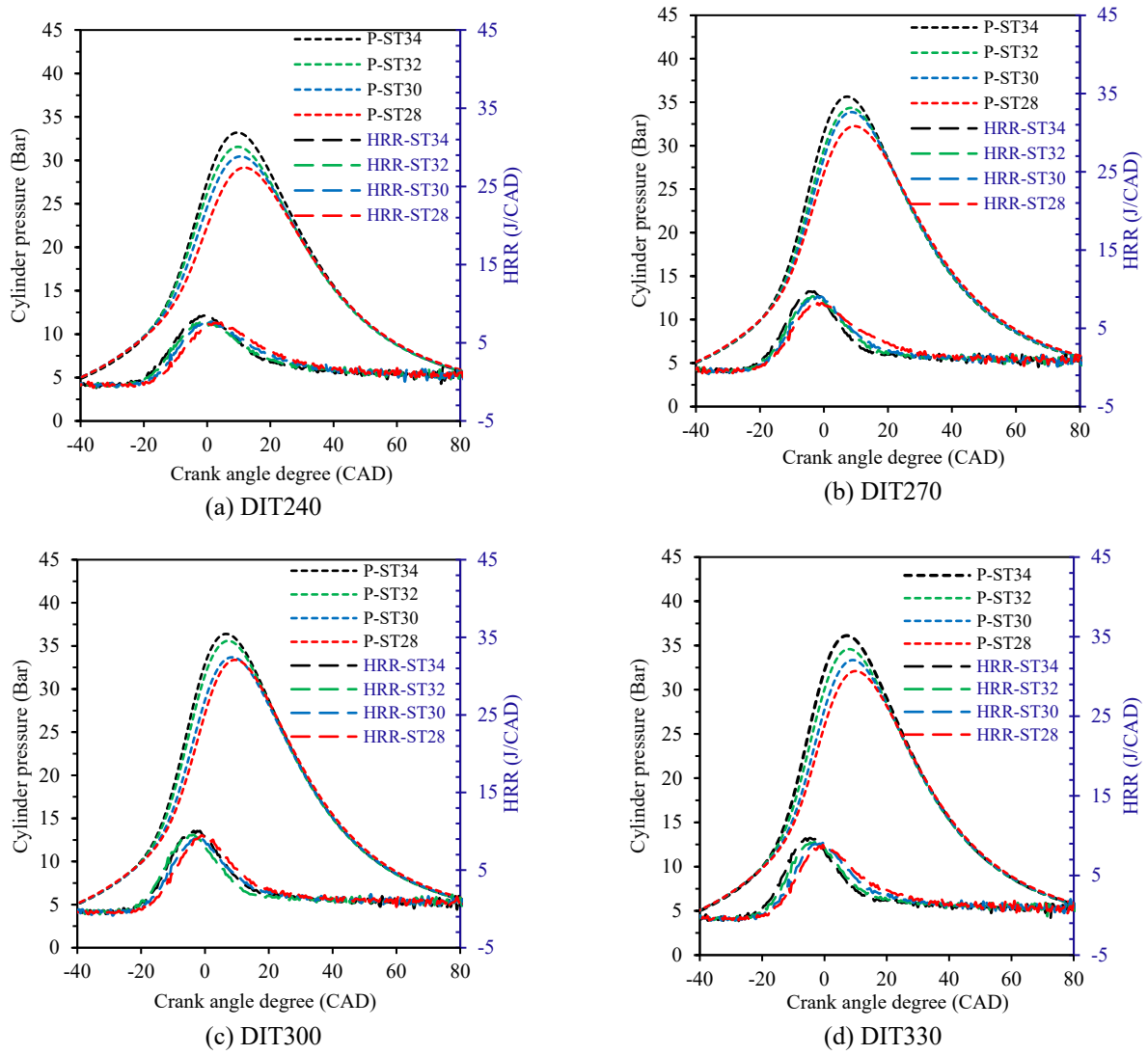

Figure 3. Combustion pressure and heat release rate variation with spark and DI timings.

Emissions Performance and Characteristics at MBT Window

Figure 4(a) and 4(b) show the variation of the ISCO and ISHC with the DI and spark timings. The ISCO and ISHC significantly decrease when DI timing is advanced from DIT240 and DIT330. When spark timing is advanced at each of these DI timings, the ISCO and ISHC potentially decrease. However, at DIT270 and DIT300, the ISCO remarkably increases with advanced spark timing until ST32 and then it decreases when the spark timing is further advanced to ST34. This performance could be attributed to the severe fuel impingement to the combustion chamber walls caused by smaller combustion chamber volume when the DI timing is advanced toward DIT270 and DIT300. This could be combined with the decreased temperature of the combustion chamber walls and residuals inside. Therefore, strong fuel impingement could result in fuel film regions that are rich and have a slow vaporisation speed [33]. The best ISCO and ISHC emissions performance are shown at DIT330 through all the tested spark timings. The early DI timing, DIT330, provides sufficient time for the spray's droplets to complete the evaporation process before the start of the combustion. Moreover, the recycled hot residuals might increase the vapour pressure of the droplets, which helps in completing air-fuel homogenisation.

In addition, the combustion chamber walls, which is still warm, could enhance the evaporation of the impinged fuel. Consequently, the air-fuel mixture could be evenly distributed inside the combustion chamber so that the local rich regions could be avoided [5]. This might partly explain the significant reduction in the ISCO and ISHC emissions when DI timing is DIT240 and DIT330. On the other hand, as a consequence of the combustion quality improvement and HRR increment, the ISNO shows the maximum values at DIT330, as shown in Figure 4(c). It was reported that the NO emission in the exhaust tailpipe significantly related to the combustion temperature and the oxygen content in the used fuel [3].

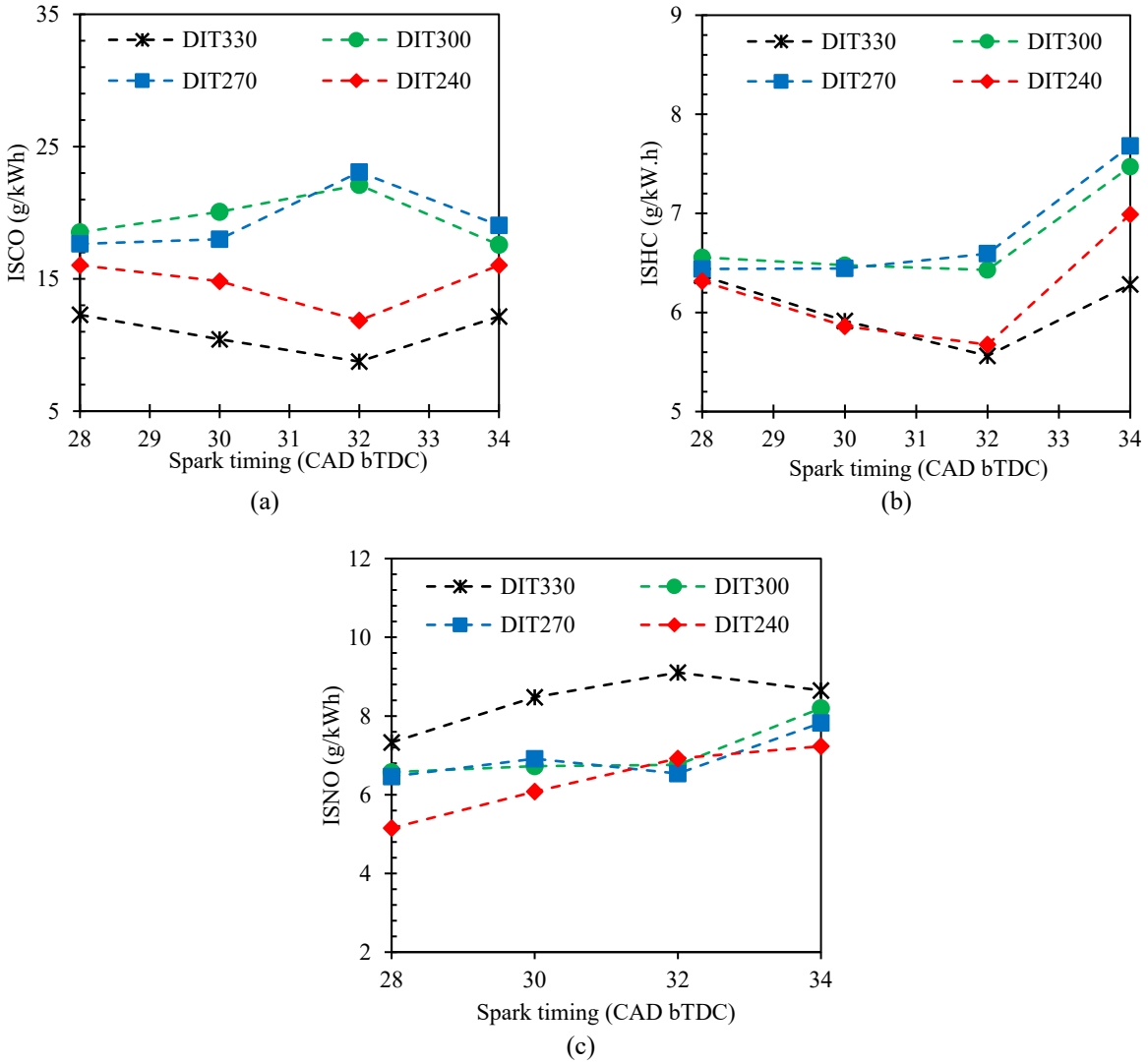

Figure 4. ISCO (a), ISHC (b) and ISNO (c) variation with spark and DI timings.

DualEI Engine Performance at the MBT Timing

The experimental results and analysis show that DI and spark timings significantly affect the DualEI engine performance, combustion and emissions characteristics. It is found that the DIT330 show superior engine performance than that of DIT240, DIT270, and DIT300 at the same engine operating conditions and input heating value. The best engine performance for minimum exhaust emissions are recorded at DI timing of DIT330, and minimum spark timing of ST30, at light load. This section will evaluate the engine performance, combustion and emission characteristics at that MBT timing.

Figure 5(a) shows the effect of DI ratio on IMEP of the DualEI engine at the MBT timing. At both engine speeds, the IMEP slightly increases when the DI ratio is increased from 0.0% until it reaches around 60%. The maximum increment of the IMEP is 6.38% when the IMEP increases from 0.460 MPa at DI0% to 0.465 MPa at DI60%, at 3500 RPM. Injecting up to 50% of the used fuel directly inside the combustion chamber by using the DI strategy could significantly enhance the mixture quality. This could be mainly attributed to the cooling effect of the ethanol directly injected which could significantly reduce the convective heat losses through cylinder walls. Furthermore, the finer fuel droplet due to the high-pressure DI system might significantly promote the poor evaporation rate of ethanol by increasing the contact surface area with ambient [34]. Moreover, the portion of the fuel directly injected may utilise the hot residuals and the combustion chamber walls. This could significantly enhance the mixture quality and then the engine performance.

However, the IMEP significantly decreases when the DI ratio is further increased to DI100%. Sever fuel impingement to combustion chamber walls could be the main reason behind this decrement. Moreover, the overcooling effect caused by a large amount of fuel directly injected associated with severe fuel impingement may create local rich mixture regions [17]. Consequently, uneven mixture distribution inside the chamber might happen, and unevaporated fuel droplets could be left as unburned particles. This could result in a lean mixture around spark plus resulting in poor quality and unstable combustion. Moreover, the peak combustion pressure (Pmax) slightly decreases at 3500 RPM, but it significantly reduces at 4000 RPM by about 8.32% when the DI ratio is increased from DI0% to DI100%, as shown in Figure 5(b). Furthermore, at 4000 RPM, the engine volumetric efficiency remarkably increases by about 4.04% when the DI ratio is increased from DI0% to DI100%, as shown in Figure 5(c). These results might be attributed to the cooling effect of the DI strategy associated with the great latent heat of vaporisation of ethanol fuel. Injecting fuel directly into the cylinder might allow

the fuel droplets to absorb more heat from the gas inside the combustion chamber instead of the intake port, and thus reduces the mixture temperature significantly. This is shown in Figure 5(b) when the Pmax significantly reduces with increased DI ratio while the IMEP remains almost the same or slightly decreases, as shown in Figure 5(a). The combustion pressure reduction might significantly reduce the combustion temperature when the DI ratio is increased. The mechanism behind the combustion temperature reduction caused by ethanol DI strategy was numerically investigated and explained in reference [8]. As a result, a significant Pmax reduction at approximately constant IMEP or slightly increased could provide more room to increase the intake pressure and thus improve the engine output power. Moreover, a great possibility of implementing the engine downsizing concept to the DualEI engine with less possible hardware limits is caused by high combustion pressure, temperature and knock. Furthermore, as shown in Figure 5(d), the COV_{IMEP} for all conditions is less than 4%, which is in the accepted range of combustion stability [31].

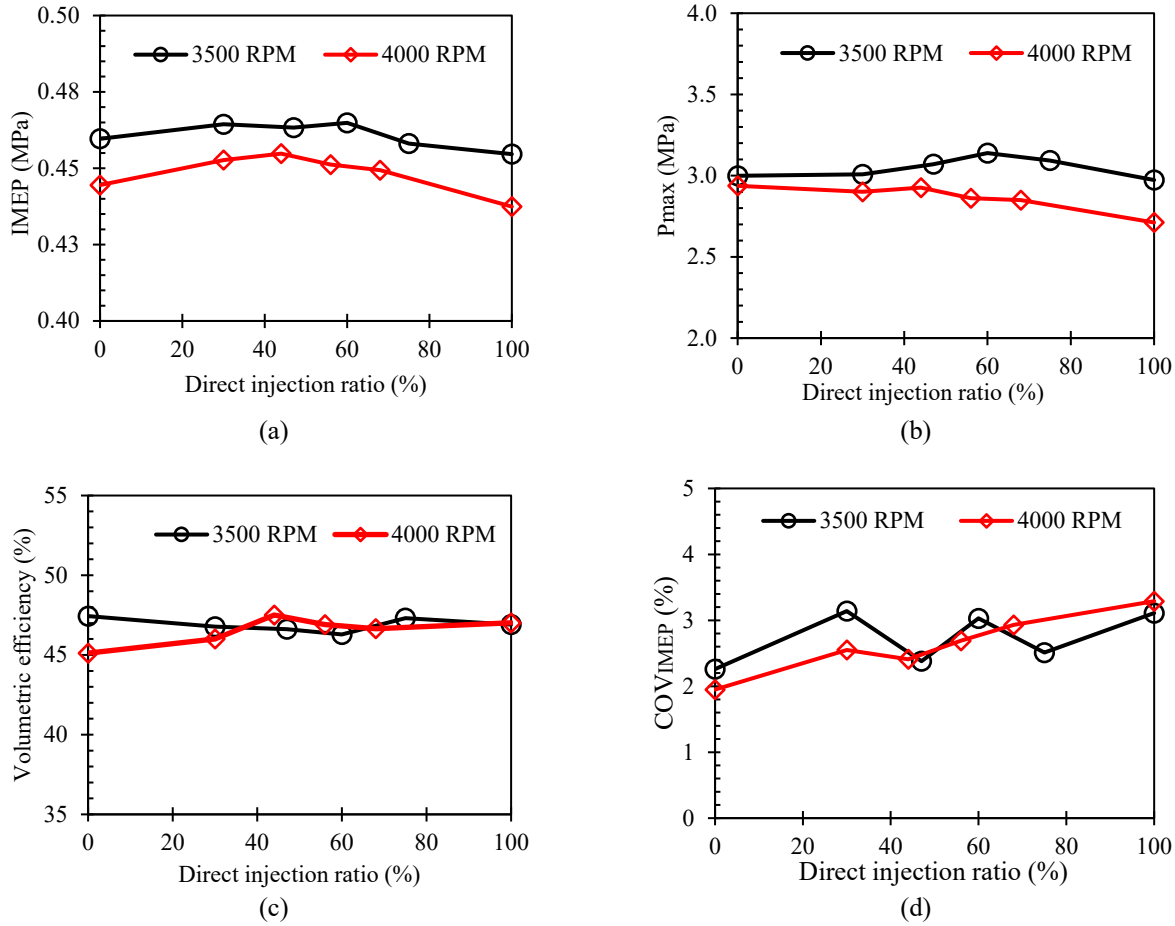

Figure 5. The IMEP (a), Pmax (a), volumetric efficiency (c) COV_{IMEP}, and (d) variation with the DI ratio.

Exhaust Emissions Characteristics of DualEI Engine at MBT Timing

Figure 6(a) and 6(b) shows the ISCO and ISHC variation with DI and spark timings at 3500 and 4000 RPM engine speed. The ISCO and ISHC slightly increase when the DI ratio is increased from DI0% to around DI60%. However, the ISCO and ISHC sharply increase when the DI ratio is further increased until it reaches DI100%. This performance could be attributed to the severe fuel impingement of DI strategy to the combustion chamber walls. Consequently, fuel film formation on the chamber walls might be created, resulting in over-rich mixture regions near the cylinder liner and piston crevice. Furthermore, uneven mixture distribution might create a lean mixture around the spark plug resulting in slow initial flame speed and thus time shortage to consume all the fuel inside the combustion chamber. The overcooling effect of the DI strategy could be another reason behind the CO and HC increment in exhaust emission.

On the other hand, ISNO emission significantly reduces when the DI ratio is increased, as shown in Figure 6(c). Consequently, the poor quality and overcooling effect might lead to an increase in the ISCO and ISHC emissions, but they significantly reduce the ISNO emissions due to their strong relation to the combustion temperature [3, 31]. Moreover, the significant reduction in combustion pressure and temperature contributes considerably to the ISNO decrement when the DI ratio is increased from DI0% to DI100%.

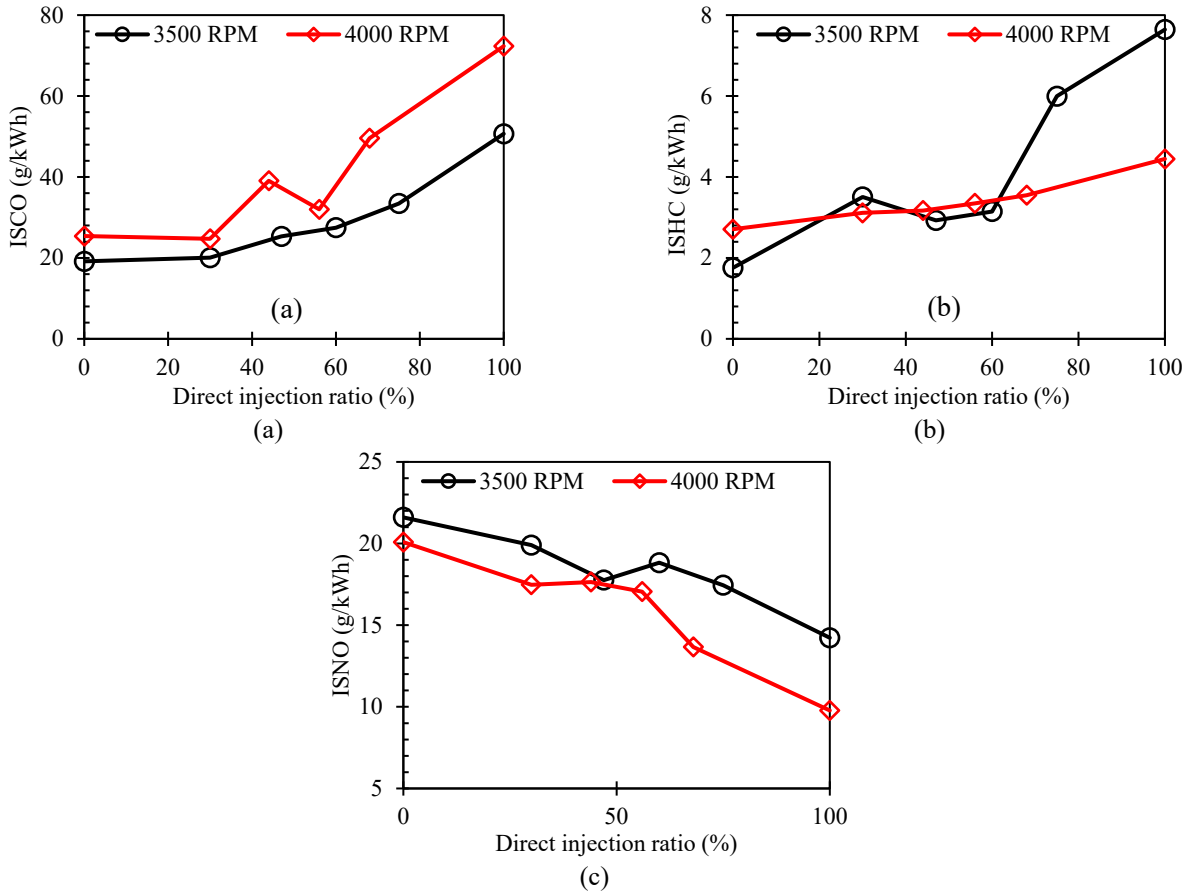

Figure 6. The ISCO (a), ISHC (b) and ISNO (c) variation with the direct injection ratio.

CONCLUSION

Experiments were carried out to determine the optimal operating position (MBT timing) at DI and spark timings window to a naturally aspirated SI engine equipped with a DualEI system. At 3500 RPM, DI timing was varied from DI240 to DIT330 at 30 CAD intervals. At each DI timing, the spark timing was advanced from ST28 to ST34 at light engine load. The effect of the DI and spark timings on the combustion and emissions characteristics was presented and analysed. The MBT timing that produced the maximum output power while the minimum emissions were used to investigate the effect of the DI ratio on the DualEI engine. The results of this study can be concluded as follows.

i. At the MBT timing window, the DIT330 showed superior engine performance and combustion quality for all the tested spark timings. At spark timing of ST30, the IMEP increased by 1.52% and 2.57% compared to DIT270 and DIT300, respectively. Moreover, the COV_{IMEP} significantly reduced when the DI timing was advanced from DIT240 to DIT330. At DIT330, the minimum COV_{IMEP} was found 2.82% and 2.77% at ST30 and ST32, respectively. However, the effect of advanced spark timing was adversely affected the engine IMEP and indicated thermal efficiency due to the negative work. Therefore, the ST30 was selected as the minimum spark advance to produce the maximum output power at DIT330.

ii. Consistently with engine performance results, the DIT330 showed the best combustion and emission quality for all the tested spark timings. Compared to ST28, the combustion efficiency increased by up to 7.29% and 11.19% at ST30 and ST32, respectively. Moreover, the ISCO and ISHC were minimum when the DIT330 was used. The ISCO decreased by 15.07% and ISHC by 7.16% at ST30, compared to ST28. However, the ISNO significantly increased by up to 15.67% when the spark timing was advanced. Furthermore, at ST30, advancing DI timing from DIT240 to DIT330 could also increase the ISNO emission by up to 6.95%. The NO results were attributed to the combustion quality improvement when the DI and ST timings were advanced.

iii. At the MBT timing, the IMEP and indicated thermal efficiency slightly increased when the DI ratio was increased from DI0% to around DI60%. Compared to port injection only, the IMEP increased by 1.13% and 1.51% at 3500 and 4000 RPM, respectively, when the DI ratio increased from DI0% to around DI60%. However, the IMEP and indicated thermal efficiency slightly decreased when the DI ratio further increased to DI100%. Furthermore, at 4000 RPM, the COV_{IMEP} slightly increased from 1.95% to 3.29% when the DI ratio was increased from DI0% to DI100%. However, for the tested conditions, the COV_{IMEP} results were less than 5.0%, which showed acceptable combustion stability through all the engine tested conditions.

iv. The ISCO and ISHC were significantly increased when the DI ratio increased from DI% to DI100%. However, the ISNO was substantially decreased with an increased DI ratio caused by the cooling effect of the DI strategy.

ACKNOWLEDGMENT

The scholarship provided by the Iraqi Ministry of Higher Education & Scientific Research is gratefully appreciated.

REFERENCES

[1] European Parliament and of the Council of 20 June 2007 on type approval of motor vehicles with respect to emissions from light passenger and commercial vehicles (Euro 5 and Euro 6) and on access to vehicle repair and maintenance information (Text with EEA relevance), EUR-Lex Regulation (EC) No 715/2007, 2007.

[2] P. Bajpai, *Advances in Bioethanol*, 2013 ed. India: Springer New Delhi Heidelberg New York Dordrecht London (in English), 2013.

[3] B. M. Masum *et al.*, "Effect of ethanol–gasoline blend on NOx emission in SI engine," *Renew. Sustain. Energy Rev.*, vol. 24, pp. 209-222, 2013, doi: 10.1016/j.rser.2013.03.046.

[4] C. L. Yaws, "Yaws' Handbook of thermodynamic and physical properties of chemical compounds: Physical, thermodynamic and transport properties for 5,000 organic chemical compounds," *USA: Knovel*, 2003.

[5] R. D. Reitz, "Directions in internal combustion engine research," *Combust. Flame,* vol. 160, no. 1, pp. 1-8, 2013, doi: 10.1016/j.combustflame.2012.11.002.

[6] J. W. G. Turner *et al.* "Alcohol-based fuels in high performance engines," *SAE Tech. Pap.*, 2007-01-0056, 2007, doi: 10.4271/2007-01-0056.

[7] M. Koç, Y. Sekmen, T. Topgül, and H. S. Yücesu, "The effects of ethanol–unleaded gasoline blends on engine performance and exhaust emissions in a spark-ignition engine," *Renew. Energy*, vol. 34, no. 10, pp. 2101-2106, 2009, doi: 10.1016/j.renene.2009.01.018.

[8] Y. Huang, G. Hong, and R. Huang, "Numerical investigation to the dual-fuel spray combustion process in an ethanol direct injection plus gasoline port injection (EDI+GPI) engine," *Energy Convers. Manag.*, vol. 92, pp. 275-286, 2015, doi: 10.1016/j.enconman.2014.12.064.

[9] Y. Huang *et al.*, "Spray and evaporation characteristics of ethanol and gasoline direct injection in non-evaporating, transition and flash-boiling conditions," *Energy Convers. Manag.*, vol. 108, pp. 68-77, 2016, doi: 10.1016/j.enconman.2015.10.081.

[10] C. M. Engler-Pinto and L. de Nadai, "Volumetric efficiency and air-fuel ratio analysis for flex fuel engines," *SAE Tech. Pap.*, 2008-36-0223, 2008, doi: 10.4271/2008-36-0223.

[11] J. W. G. Turner, A. Peck, and R. J. Pearson, "Flex-fuel vehicle development to promote synthetic alcohols as the basis of a potential negative-CO_2 energy economy," *SAE Tech. Pap.*, 2007-01-3618, 2007, doi: 10.4271/2007-01-3618.

[12] K. Nakata *et al.*, "The effect of ethanol fuel on a spark ignition engine," *SAE Tech. Pap.*, 2006-01-3380, 2006, doi: 10.4271/2006-01-3380.

[13] M. Pontoppidan and F. Damasceno, "The integral flex-vehicle mixture control of alcohol-based bio-fuels - a new challenge for fuel-atomizer optimization," *SAE Tech. Pap.*, 2008-01-0437, 2008, doi: 10.4271/2008-01-0437.

[14] X. Yu *et al.*, "Effects of hydrogen direct injection on combustion and emission characteristics of a hydrogen/acetone-butanol-ethanol dual-fuel spark ignition engine under lean-burn conditions," *Int. J. Hydrog. Energy*, vol. 45, no. 58, pp. 34193-34203, 2020, doi: 10.1016/j.ijhydene.2020.09.080.

[15] H. Gürbüz *et al.*, "Effect of port injection of ethanol on engine performance, exhaust emissions and environmental factors in a dual-fuel diesel engine," *Energy & Environment*, vol. 32, no. 5, pp. 784-802, 2020, doi: 10.1177/0958305X20960701.

[16] Y. Qian *et al.*, "Co-effects of fuel research octane number and ethanol injection ratio on dual-fuel spark-ignition engine," *Int. J. Engine Res.*, vol. 22, no. 2, pp. 456-467, 2019, doi: 10.1177/1468087419866589.

[17] Y. Huang, G. Hong, and R. Huang, "Investigation to charge cooling effect and combustion characteristics of ethanol direct injection in a gasoline port injection engine," *Appl. Energy*, vol. 160, pp. 244-254, 2015, doi: 10.1016/j.apenergy.2015.09.059.

[18] Z. Chen, L. Wang, and K. Zeng, "Comparative study of combustion process and cycle-by-cycle variations of spark-ignition engine fueled with pure methanol, ethanol, and n-butanol at various air–fuel ratios," *Fuel,* vol. 254, p. 115683, 2019, doi: 10.1016/j.fuel.2019.115683.

[19] S. Kumar, N. Singh, and R. Prasad, "Anhydrous ethanol: A renewable source of energy," *Renew. Sustain. Energy Rev.*, vol. 14, no. 7, pp. 1830-1844, 2010, doi: 10.1016/j.rser.2010.03.015.

[20] S. Taniguchi, K. Yoshida, and Y. Tsukasaki, "Feasibility study of ethanol applications to a direct injection gasoline engine," *SAE Tech. Pap.*, 2007-01-2037, 2007. doi: 10.4271/2007-01-2037.

[21] A. Boretti, "Analysis of design of pure ethanol engines," *SAE Tech. Pap.*, 2010-01-1453, 2010, doi: 10.4271/2010-01-1453.

[22] N. F. O. Al-Muhsen, J. Wang, and G. Hong, "Investigation to combustion and emission characteristics of the dual ethanol injection spark ignition engine," in *20th Australasian Fluid Mechanics Conference*, 2016.

[23] Y. Zhuang and G. Hong, "Effects of direct injection timing of ethanol fuel on engine knock and lean burn in a port injection gasoline engine," *Fuel*, vol. 135, no. 2014, pp. 27-37, 11/1/2014 2014, doi: http://dx.doi.org/10.1016/j.fuel.2014.06.028.

[24] Y. Zhuang and G. Hong, "Primary investigation to leveraging effect of using ethanol fuel on reducing gasoline fuel consumption," *Fuel*, vol. 105, no. 2013, pp. 425-431, 2013, doi: http://dx.doi.org/10.1016/j.fuel.2012.09.013.

[25] G. Zhu, D. Hung, and H. Schock, "Combustion characteristics of a single-cylinder spark ignition gasoline and ethanol dual-fuelled engine," *Proc. Inst. Mech. Eng. D: Int. J. Automot. Eng.,* vol. 224, no. 3, pp. 387-403, 2010, doi: 10.1243/09544070JAUTO1236.

[26] Y. Huang *et al.*, "The effect of fuel temperature on the ethanol direct injection spray characteristics of a multi-hole injector," *SAE Int. J. Fuels Lubr.*, vol. 7, no. 3, pp. 792-802, 2014, doi: 10.4271/2014-01-2734.

[27] B. Motorsport, "HP Injection Valve HDEV 5.2," [Online] Available: http://www.bosch-motorsport.com/media/catalog_resources/HP_Injection_Valve_HDEV_52_Datasheet_51_en_2776067211pdf. [Accessed: Jan. 13, 2018]

[28] N. F. O. Al-Muhsen, Y. Huang, and G. Hong, "Effects of direct injection timing associated with spark timing on a small spark ignition engine equipped with ethanol dual-injection," *Fuel*, vol. 239, pp. 852-861, 2019, doi: 10.1016/j.fuel.2018.10.118.

[29] Y. Zhuang, Y. Qian, and G. Hong, "The effect of ethanol direct injection on knock mitigation in a gasoline port injection engine," *Fuel*, vol. 210, pp. 187-197, 2017, doi: 10.1016/j.fuel.2017.08.060.

[30] N. F. O. Al-Muhsen and G. Hong, "Effect of spark timing on performance and emissions of a small spark ignition engine with dual ethanol fuel injection," *SAE Tech. Pap.*, 2017-01-2230, 2017. doi: 10.4271/2017-01-2230.
[31] J. B. Heywood, *Internal combustion engine fundamentals. McGraw-Hill, Inc. (in English)*, 1988, p. 930.
[32] W. Zeng *et al.,*"Atomisation and vaporisation for flash-boiling multi-hole sprays with alcohol fuels," *Fuel*, vol. 95, pp. 287-297, 2012, doi: 10.1016/j.fuel.2011.08.048.
[33] F. Schulz *et al.*, "Gasoline wall films and spray/wall interaction analysed by infrared thermography," *SAE Int. J. Engines*, vol. 7, no. 3, pp. 1165-1177, 2014, doi: 10.4271/2014-01-1446.
[34] P. Sementa, B. M. Vaglieco, and F. Catapano, "Influence of the injection pressure on the combustion performance and emissions of small gdi engine fuelled with bio-ethanol," *SAE Tech. Pap.*, 2011-37-0007, 2011, doi: 10.4271/2011-37-0007.